Combined targeting of HER2 and VEGFR2 for effective treatment of *HER2*-amplified breast cancer brain metastases

David P. Kodack[a,1], Euiheon Chung[a,b,1], Hiroshi Yamashita[a,1], Joao Incio[a], Annique M. M. J. Duyverman[a], Youngchul Song[c], Christian T. Farrar[d], Yuhui Huang[a], Eleanor Ager[a], Walid Kamoun[a], Shom Goel[a], Matija Snuderl[a,e], Alisha Lussiez[a], Lotte Hiddingh[a], Sidra Mahmood[a], Bakhos A. Tannous[f], April F. Eichler[g], Dai Fukumura[a,2], Jeffrey A. Engelman[c,2], and Rakesh K. Jain[a,2]

[a]Edwin L. Steele Laboratory for Tumor Biology, Department of Radiation Oncology, [c]Department of Medicine, [d]Martinos Center for Biomedical Imaging, [e]Department of Pathology, [f]Department of Neurology, and [g]Stephen E. and Catherine Pappas Center for Neuro-Oncology, Massachusetts General Hospital and Harvard Medical School, Boston, MA 02114; and [b]Department of Medical System Engineering and School of Mechatronics, Gwangju Institute of Science and Technology, Gwangju 500-712, South Korea

Contributed by Rakesh K. Jain, September 17, 2012 (sent for review June 10, 2012)

Brain metastases are a serious obstacle in the treatment of patients with *human epidermal growth factor receptor-2* (*HER2*)–amplified breast cancer. Although extracranial disease is controlled with HER2 inhibitors in the majority of patients, brain metastases often develop. Because these brain metastases do not respond to therapy, they are frequently the reason for treatment failure. We developed a mouse model of *HER2*-amplified breast cancer brain metastasis using an orthotopic xenograft of BT474 cells. As seen in patients, the HER2 inhibitors trastuzumab and lapatinib controlled tumor progression in the breast but failed to contain tumor growth in the brain. We observed that the combination of a HER2 inhibitor with an anti–VEGF receptor-2 (VEGFR2) antibody significantly slows tumor growth in the brain, resulting in a striking survival benefit. This benefit appears largely due to an enhanced antiangiogenic effect: Combination therapy reduced both the total and functional microvascular density in the brain xenografts. In addition, the combination therapy led to a marked increase in necrosis of the brain lesions. Moreover, we observed even better antitumor activity after combining both trastuzumab and lapatinib with the anti-VEGFR2 antibody. This triple-drug combination prolonged the median overall survival fivefold compared with the control-treated group and twofold compared with either two-drug regimen. These findings support the clinical development of this three-drug regimen for the treatment of *HER2*-amplified breast cancer brain metastases.

treatment resistance | tumor–stroma interaction | targeted therapy | tumor microenvironment | antiangiogenesis

Approximately 25% of human breast cancers demonstrate amplification of the *human epidermal growth factor receptor-2* (*HER2*) protooncogene. Patients with HER2-positive breast cancer are at a high risk of developing brain metastases, with a frequency as high as 50% in patients succumbing to advanced disease (1–4). A combination of factors explains this phenomenon, including the proclivity of HER2-positive tumor cells to colonize the brain and improved control of extracranial disease with the anti-HER2 monoclonal antibody trastuzumab (Genentech/Roche) enabling patients to live long enough to develop brain metastases (1, 5). Although systemic disease is under control in many of these patients, their associated brain metastases appear resistant to trastuzumab (2, 6, 7). Furthermore, lapatinib (GlaxoSmithKline), a small-molecular-weight HER2 kinase inhibitor, thought to penetrate the blood–brain barrier better compared with trastuzumab, has shown only a modest response in patients with recurrent or progressive brain metastases (8–10). Thus, alternative strategies are desperately needed to treat patients with metastatic disease (11).

Angiogenesis is critical to breast cancer progression and metastasis, and adversely affects prognosis (12, 13). VEGF is one of the most potent angiogenic factors (14). In patients with metastatic breast cancer, the anti-VEGF antibody bevacizumab (Genentech/Roche), in combination with paclitaxel, prolonged progression-free survival but not overall survival compared with paclitaxel alone (15). In addition, the use of bevacizumab with trastuzumab and chemotherapy in HER2-positive metastatic breast cancer has shown some promise in phase II trials (16). However, there remain no data on the efficacy of bevacizumab in the context of brain metastases because these patients have often been excluded from clinical trials due to fear of an increased risk of cerebral hemorrhage after anti-VEGF therapy. However, retrospective analysis has shown this potential risk may not be significant (17). Currently, clinical trials are underway to evaluate the efficacy of bevacizumab in patients with breast cancer who have active brain metastases, including its combination with trastuzumab in patients with HER2-positive disease (http://clinicaltrials.gov identifier NCT01004172). However, the effects of dual blockade of VEGF and HER2 in brain metastases have not been examined in preclinical models.

We have previously shown that trastuzumab alone can act as an antiangiogenic mixture in a leptomeningeal metastasis model of HER2-overexpressing breast cancer through a reduction in proangiogenic factors and an increase in an antiangiogenic factor (18). These effects were transient, however, and were counteracted by the compensatory production of VEGF from host stromal cells, perhaps to rescue angiogenesis. Indeed, carcinoma-associated fibroblasts as well as immune cells can produce significant amounts of VEGF in breast cancer models (19, 20). These findings suggest that blockade of the VEGF pathway may overcome trastuzumab resistance by inhibiting the activity of the

Author contributions: D.P.K., E.C., H.Y., J.I., A.M.M.J.D., D.F., J.A.E., and R.K.J. designed research; D.P.K., E.C., H.Y., J.I., A.M.M.J.D., Y.S., C.T.F., Y.H., E.A., S.G., A.L., L.H., and S.M. performed research; B.A.T. contributed new reagents/analytic tools; D.P.K., E.C., H.Y., J.I., A.M.M.J.D., W.K., M.S., A.F.E., D.F., J.A.E., and R.K.J. analyzed data; and D.P.K., E.C., H.Y., D.F., J.A.E., and R.K.J. wrote the paper.

Conflict of interest statement: J.A.E. serves as a consultant for GlaxoSmithKline and Genentech (Roche). R.K.J. has research grants from Dyax, MedImmune, and Roche; serves as a consultant to Noxxon Pharmaceuticals; serves on the Scientific Advisory Board of Enlight and SynDevRx; serves on the Board of Directors of XTuit; serves on the Board of Trustees of H&Q Healthcare Investors and H&Q Life Sciences Investors; and has equity in Enlight, SynDevRx, and XTuit Pharmaceuticals. No funds or reagents from any of these organizations were used in the current study.

Freely available online through the PNAS open access option.

[1]D.P.K., E.C., and H.Y. contributed equally to this work.

[2]To whom correspondence may be addressed. E-mail: dai@steele.mgh.harvard.edu, jengelman@partners.org, or jain@steele.mgh.harvard.edu.

See Author Summary on page 18261 (volume 109, number 45).

This article contains supporting information online at www.pnas.org/lookup/suppl/doi:10.1073/pnas.1216078109/-/DCSupplemental.

compensatory VEGF production by stromal cells, resulting in a significantly greater antiangiogenic effect. This hypothesis is consistent with the finding that targeting both HER2 and VEGF in orthotopic breast cancer xenografts results in better growth delay than targeting either agent alone (21, 22). Furthermore, the phase II study of bevacizumab in combination with trastuzumab and capecitabine as first-line treatment for HER2-positive locally recurrent or metastatic breast cancer showed an overall response rate of 73% (16).

Herein, we developed a model of *HER2*-amplified breast cancer brain metastases. Although the brain metastases were resistant to single-agent lapatinib or trastuzumab, we observed that the combination of trastuzumab, lapatinib, and an anti-murine VEGFR2 antibody, DC101 [ImClone Systems/Eli Lilly and Company (23)], resulted in a markedly delayed progression of these brain metastases. These studies point to a new therapeutic approach for patients with *HER2*-amplified breast cancer brain metastases.

Results

Mouse Model That Recapitulates the Differential Response of Intracranial and Extracranial *HER2*-Amplified Breast Cancers to HER2 Inhibitors. We used a previously established technique to monitor metastatic tumor growth sensitively and noninvasively in the brain in real-time (24). *HER2*-amplified BT474 cells were infected with a lentivirus leading to expression of both *Gaussia* luciferase (Gluc) and cerulean fluorescent protein (CFP). This facilitates noninvasive monitoring of BT474-Gluc tumor growth in the brain parenchyma after direct injection (*a*) by measuring Gluc activity in the bloodstream (Gluc is secreted by tumor cells into the bloodstream) and (*b*) through the cranial window using intravital fluorescence microscopy, respectively. Fig. 1*A* illustrates a brain metastatic lesion as seen with bioluminescence imaging and intravital multiphoton microscopy. The BT474-Gluc brain lesion depicted by bioluminescence represents the approximate tumor size on initiation of treatment (Fig. 1*A*, *Left*). Intravital multiphoton microscopy illustrates the brain lesion boundary (Fig. 1*A*, *Center*) and the abnormality of the tumor vasculature (Fig. 1*A*, *Right*). Blood Gluc activity correlated well with BT474-Gluc tumor volume as measured by intravital microscopy (Fig. S1*A*). Blood Gluc activity also correlated with tumor volume measured using MRI and bioluminescence (Fig. S1 *B* and *C*). Furthermore, analysis of tumor volume ex vivo using multispectral fluorescent imaging supports the correlation between blood Gluc activity and tumor volume (Fig. S1*D*). Thus, blood Gluc activity was used to monitor tumor size and response to treatment.

We first tested the effects of anti-HER2 therapies on the growth of established BT474-Gluc tumors growing in the mammary fat pad (primary) and in the brain parenchyma (metastases). Treatment was initiated when brain metastatic tumors reached ~10 mm^3 in volume [corresponding to a blood Gluc activity of 10 Relative Light Units per second (RLU/s)], as illustrated in Fig. 1*A*. Although BT474-Gluc tumors in the mammary

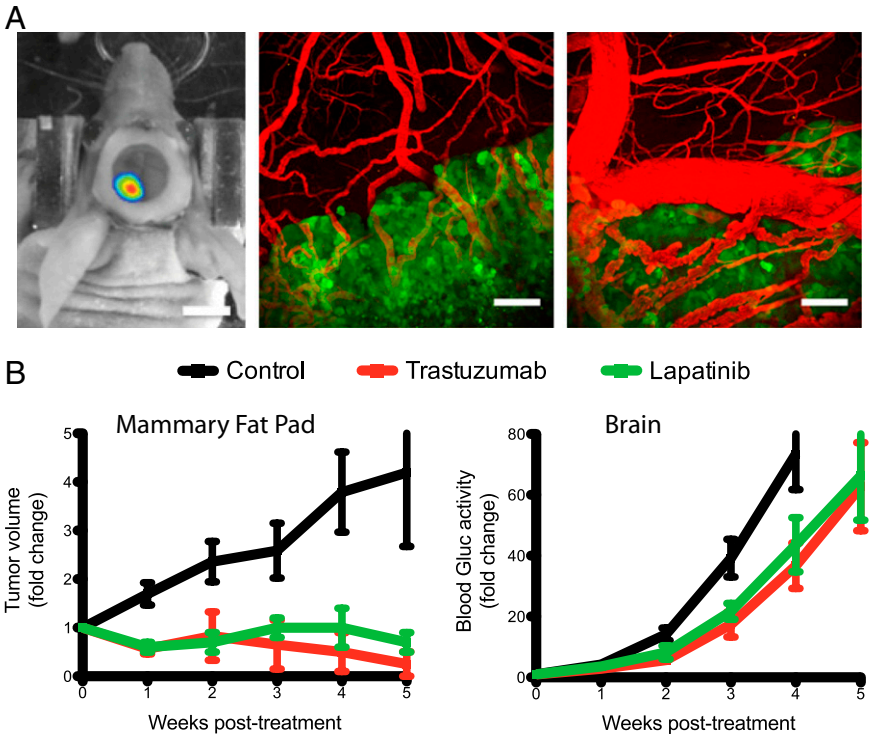

Fig. 1. Imaging of the breast cancer brain metastasis model and the effect of anti-HER2 therapies on tumor growth. (*A*) Imaging of an established BT474-Gluc tumor after direct injection into the brain parenchyma. The cranial window was used for intravital microscopy. (*Left*) Representative bioluminescence image of the tumor symbolizes its approximate size at treatment initiation. (Scale bar: 5 mm.) Intravital multiphoton microscopy images illustrate the brain metastatic lesion boundary (*Center*) and the abnormality of the tumor vasculature (*Right*). (Scale bars: 100 μm.) Tumor cells expressing CFP are green, and blood vessels (red) are contrast-enhanced by i.v. injection of tetramethylrhodamine dextran (2,000,000 molecular weight). (*B*) Effect of trastuzumab (red, 5 mg/kg twice a week) or lapatinib (green, 100 mg/kg daily) on the growth of BT474-Gluc breast cancer cells when growing in the mammary fat pad (*Left*) or brain parenchyma (*Right*). Tumor growth curves for each treatment group are shown. Data are expressed as the mean ± SEM. (*Left*) BT474-Gluc mammary fat pad tumors were allowed to reach ~75 mm^3 in volume before treatment initiation; the *y* axis is the fold-change of tumor volume (n = 6–8 mice). (*Right*) BT474-Gluc brain metastatic tumors were allowed to reach a blood Gluc activity of roughly 10 RLU/s, corresponding to a volume of ~10 mm^3, before treatment initiation; the *y* axis is the fold-change of blood Gluc activity (n = 8–13 mice). (Treatment was initiated for BT474-Gluc brain metastatic tumors at ~10 mm^3 in all subsequent experiments. Data are expressed as the mean ± SEM in all subsequent figures.)

fat pad responded well to trastuzumab or lapatinib treatment, both HER2 inhibitors failed to control BT474-Gluc tumor growth in the brain parenchyma (Fig. 1 *B* and *C*). Thus, this mouse model closely mirrors the discordant effects of therapy in patients with metastatic HER2-positive breast cancer.

Dual Inhibition of HER2 and VEGFR2 Significantly Slows Brain Metastatic Tumor Growth and Extends Mouse Survival. Based on our previous findings proposing VEGF as a mechanism of resistance to trastuzumab in *HER2*-amplified breast cancer brain metastases, we tested if the addition of an anti-VEGF pathway inhibitor to anti-HER2 therapy could control tumor growth better than anti-HER2 therapy alone (Fig. 2). Consistent with our findings above, either trastuzumab or lapatinib monotherapy slowed brain metastatic BT474-Gluc tumor growth by only a few days compared with control-treated tumors (Fig. 2 *A* and *B*, respectively). The minimal overall survival benefit of either monotherapy was consistent with its modest effect on tumor growth: trastuzumab prolonged average survival by 7 d (1.4-fold compared with control; Fig. 2*A*), and lapatinib prolonged average survival by 3 d (1.2-fold compared with control; Fig. 2*B*). At the time of euthanasia, the size of the brain metastatic tumor was consistent among mice and occupied nearly an entire hemisphere of the brain. Thus, mouse survival in our model was considered to reflect brain metastatic tumor burden. Treatment with the antimurine VEGFR2 antibody DC101 exhibited a significant delay in tumor growth, corresponding to an improvement in survival between 2.3- and 2.4-fold greater than control-treated mice (Fig. 2 *A* and *B*, respectively; $P < 0.001$). Intriguingly, the combination of trastuzumab (Fig. 2*A*) or lapatinib (Fig. 2*B*) with DC101 showed a substantial delay in BT474-Gluc brain metastatic growth. The combination of trastuzumab and DC101 prolonged mouse survival to a median of 47.5 d, almost threefold greater than control-treated mice (additional 31.5 d; $P < 0.01$ compared with DC101 monotherapy). The combination of lapatinib and DC101 prolonged mouse survival to a median of 47 d, 3.4-fold greater than control-treated mice (additional 33 d; $P < 0.001$ compared with DC101 monotherapy). The impressive tumor growth delay witnessed by the combination of trastuzumab and DC101 was confirmed using MRI (Fig. 3*A*), bioluminescent imaging (Fig. 3*B*), and postmortem ex vivo multispectral brain imaging (Fig. S2), further validating the reliability of blood Gluc activity in monitoring brain metastatic BT474-Gluc tumor growth.

Combination of Anti-HER2 and Anti-VEGFR2 Therapies Induces Tumor Necrosis Through Antivascular Effects. To investigate the mechanism(s) for the effect of the combination treatment groups, we evaluated the histology of brain metastatic tumor tissues collected after 15 d of treatment with control IgG, trastuzumab, lapatinib, DC101, or the combination of each HER2 inhibitor with DC101. Immunohistochemical analysis revealed no obvious difference in tumor cell proliferation or apoptosis in viable tumor tissue from the six different treatment groups (Fig. S3). In addition, analysis of tumor tissue collected after 4 or 8 d of treatment revealed no difference in tumor cell proliferation or apoptosis between groups. However, we found a clear difference in the necrotic fraction of tumor tissue between treatment groups after 15 d of treatment (Fig. 4 and Fig. S4). There was a significant increase in necrotic area in tumors treated with DC101

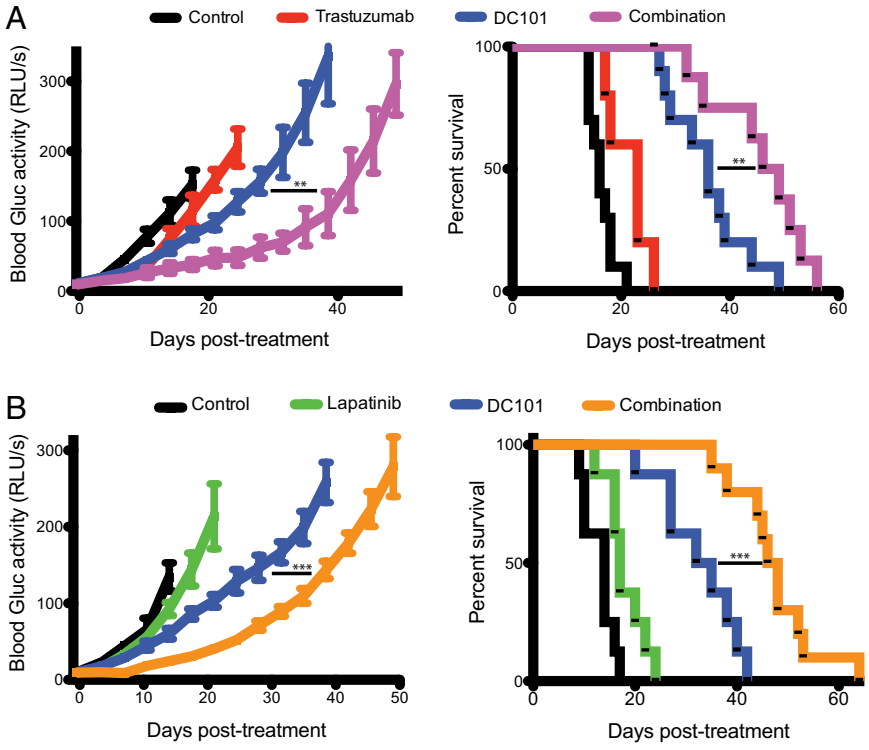

Fig. 2. Effects of anti-HER2 and anti-VEGFR2 therapies, and their combination on breast cancer growth in the brain parenchyma and mouse survival. Trastuzumab and lapatinib were dosed as previously mentioned, and DC101 was dosed at 40 mg/kg via i.p. injection twice a week. Tumor size was monitored twice a week via blood Gluc activity (*Left*), and animal survival was ascertained (*Right*). (*A*) Tumor growth plot (*Left*) and Kaplan–Meier survival plot (*Right*) of brain metastatic tumor-bearing mice treated with control (black), trastuzumab (red), DC101 (blue), or trastuzumab and DC101 (magenta) (n = 8–10 mice; except in the case of trastuzumab treatment, where n = 5 mice). $^{**}P < 0.01$. (*B*) Tumor growth plot (*Left*) and Kaplan–Meier survival plot (*Right*) of brain metastatic tumor-bearing mice treated with control (black), lapatinib (green), DC101 (blue), or lapatinib and DC101 (orange) (n = 8–10 mice). $^{***}P < 0.001$. (Final tumor growth points occur when at least 3 mice are still alive.)

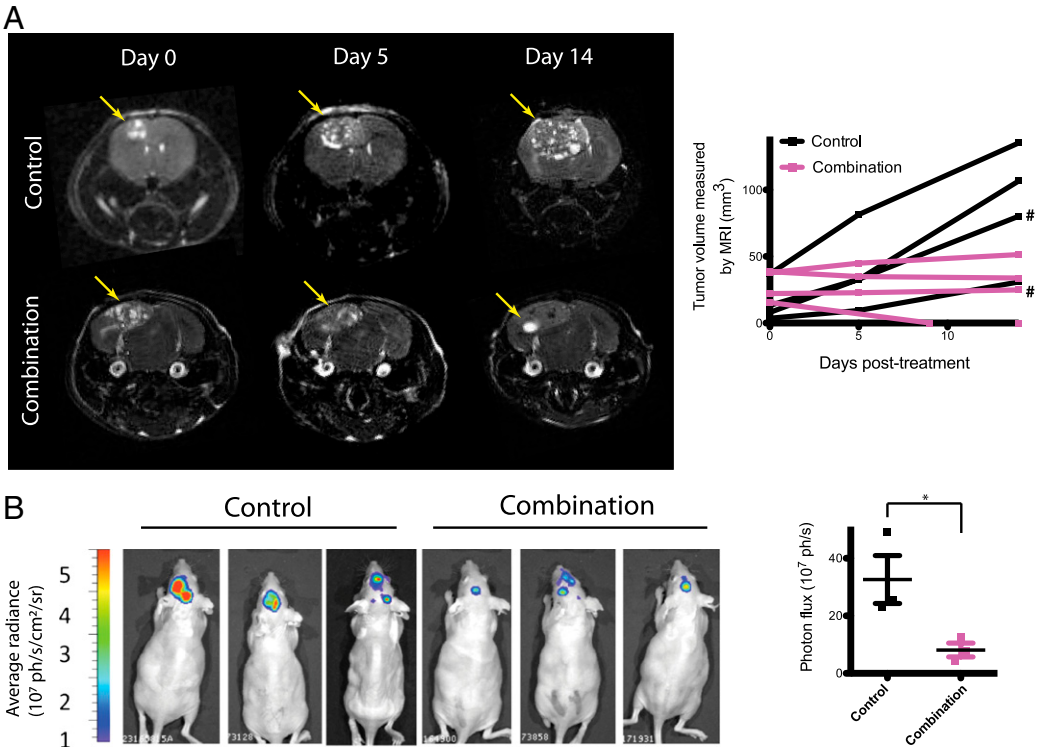

Fig. 3. Imaging of metastatic breast cancer growth in the brain parenchyma and response to the combination of anti-HER2 and anti-VEGFR2 therapy. (*A*) MRI analysis of control or trastuzumab and DC101 treatment on BT474-Gluc metastatic tumors in the brain. MRI tumor volume was measured on days 0, 5, and 14 of treatment. (*Left*) Representative MRI of control- and combination-treated tumors is shown. (*Right*) Tumor volume, calculated using MRI, is plotted for each individual mouse (# corresponds to the tumors illustrated by the MRI scans in *A*). (*B*) Bioluminescence imaging analysis of control or trastuzumab and DC101 treatment on metastatic BT474-Gluc tumors in the brain. (*Left*) Images of control- and combination-treated tumors 14 d after treatment initiation are shown. (*Right*) Average bioluminescence signal for the three control- and three combination-treated tumors is depicted. $*P < 0.05$.

compared with control- or anti-HER2–treated tumors: 7–8% in control- or anti-HER2–treated tumors vs. 21 ± 1.5% in DC101-treated tumors ($P < 0.001$). This necrotic fraction was even higher within the combination-treated tumors: 28 ± 1.8% of the tumor area in the trastuzumab and DC101-treated mice and 27 ± 1.8% in the lapatinib and DC101-treated mice ($P < 0.01$ and $P < 0.05$, respectively, compared with DC101 monotherapy). These findings indicate an enhanced antiangiogenic effect induced by the combination treatment groups, and thus led us to investigate their effects on the tumor vasculature.

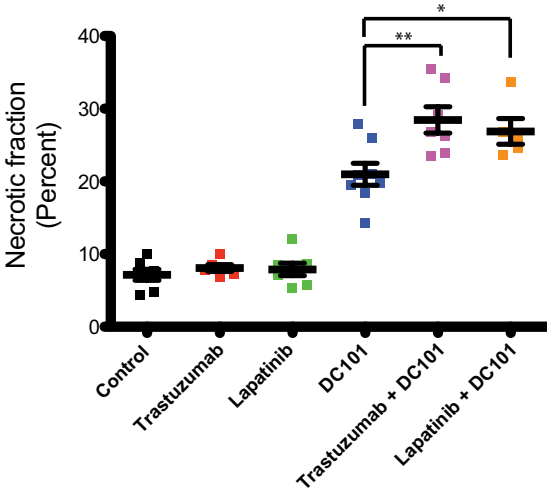

Fig. 4. Effects of the indicated treatments on the necrotic fraction of the tumor. The percentage of necrotic area in the total tumor area for each BT474-Gluc tumor was determined 15 d after treatment initiation using an in-house MATLAB program. $**P < 0.01$; $*P < 0.05$. DC101 vs. control, trastuzumab, or lapatinib ($P < 0.001$). Representative H&E-stained sections used for quantification of the necrotic area are shown in Fig. S4.

To this end, we stained brain metastatic lesions from all six treatment groups for both the endothelial cell marker CD31 and perfusion marker biotinylated-lectin, infused into the bloodstream 5 min before tumor tissue collection. HER2 inhibitors did not have a significant effect on the total or functional microvascular density (MVD) compared with control-treated tumors, which make up 5.09% and 3.88% of the viable tumor area, respectively (Fig. 5 and Fig. S5*A*). Mice treated with DC101 showed a decrease in the area of both total and functional viable tumor MVD to 2.75% and 1.84%, respectively, a decrease of ~50% compared with control-treated mice ($P < 0.001$). Finally, the combination treatments of trastuzumab and DC101 or lapatinib and DC101 revealed a steeper reduction in the total and functional tumor MVD compared with DC101 monotherapy. The combination of trastuzumab and DC101 decreased total and functional tumor MVD to 1.30% and 0.87% of viable tumor area, respectively, an approximate 75% reduction compared with control-treated tumor tissues ($P < 0.05$, compared with DC101 monotherapy). Meanwhile, the combination of lapatinib and DC101 decreased total and functional tumor MVD to 1.46% and 1.06%, respectively, an approximate 72% decrease compared with control-treated tumors ($P < 0.05$, compared with DC101 monotherapy). A similar trend was found in tumor tissues collected after 8 d of treatment (Fig. S5 *B* and *C*). These data demonstrate that combined anti-VEGFR2 and anti-HER2

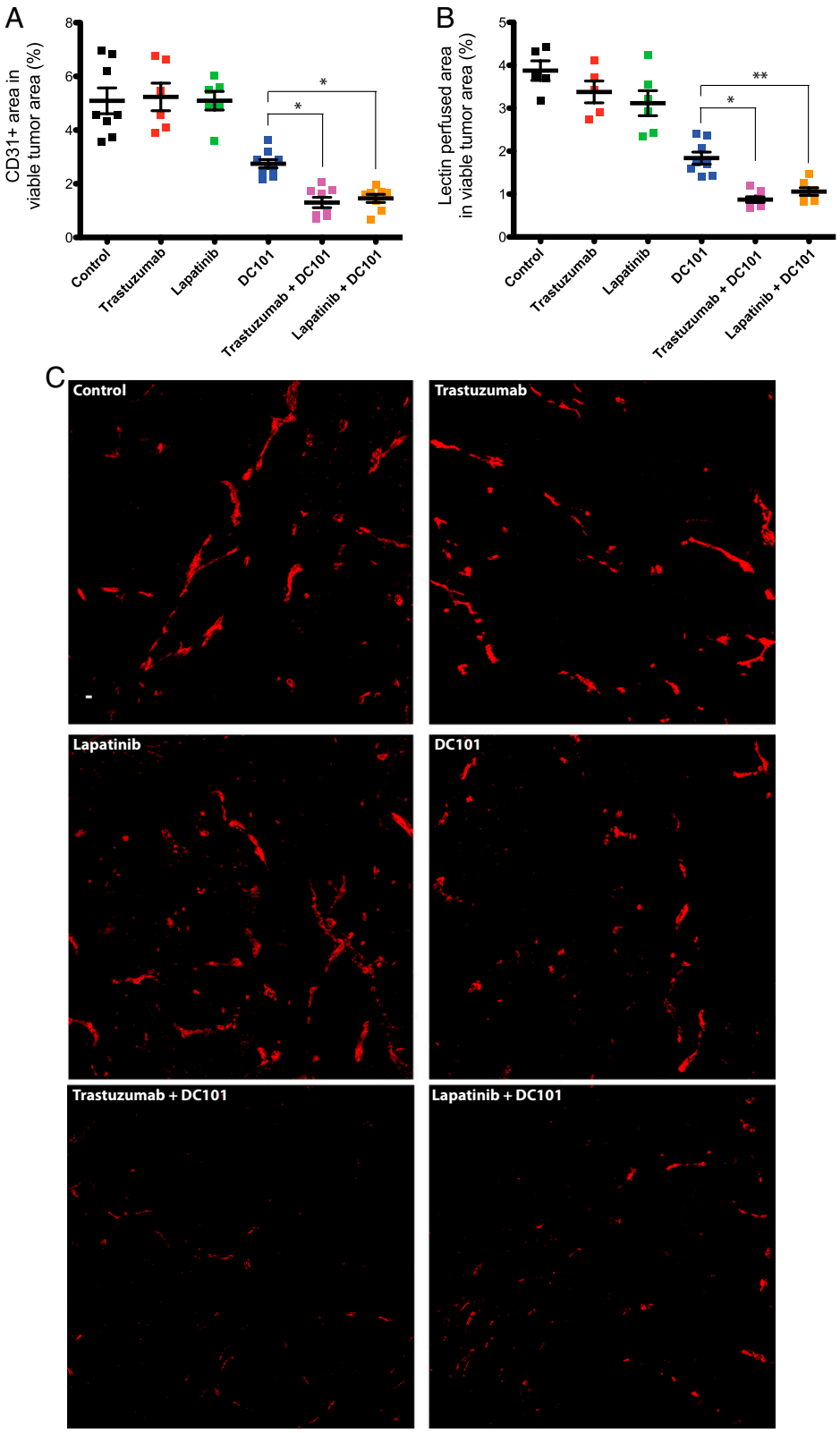

Fig. 5. Effects of the indicated treatments on blood vessels. CD31-positive blood vessel area (*A*) and lectin-positive perfused blood vessel area (*B*) in the viable regions of BT474-Gluc tumors 15 d after treatment initiation. Tissues were analyzed by an in-house MATLAB program. $*P < 0.05$; $**P < 0.01$. DC101 vs. control, trastuzumab, or lapatinib ($P < 0.001$). (*C*) Representative images of CD31-positive endothelial cells in the viable tumor tissue. (Scale bar: 100 μm.) (Representative images of lectin-positive blood vessels in the viable tumor tissue are shown in Fig. S5*A*).

therapies lead to a marked decrease in MVD and increased tumor necrosis.

Delivery of HER2 Inhibitors, NK Cell Infiltration, or Direct Tumor Cell Cytotoxicity Does Not Mediate the Reduction in Metastatic Tumor Growth Caused by the Combination of HER2 and VEGFR2 Inhibitors. We next investigated the possibility that the anti-VEGFR2 antibody augmented the capacity for the HER2 inhibitors to suppress signaling in the brain metastases. After 3 d of lapatinib, but not trastuzumab, treatment, we observed a significant decrease in phosphorylation of HER2 as well as downstream AKT and ERK in BT474-Gluc brain metastases (Fig. S6*A*). Consistent with this, after 3 d of lapatinib treatment, we found its concentration to be ∼14.5 μM within the brain metastatic tumor (Fig. S6*B*). Although this concentration is one-third of that reached in tumors growing in the mammary fat pad, it is at least 500-fold greater than the in vitro IC_{50} for this cell line (25). Interestingly, however, after 15 d of lapatinib treatment, this suppression of HER2 activation was no longer present (Fig. S7*B*). Western blot and immunohistochemical analysis showed that neither combination treatment group (neither trastuzumab and DC101 nor lapatinib and DC101) significantly altered the activation status of HER2 after 15 d of treatment, although a trend toward a modest decrease in HER2 activation was suggested (Fig. S7).

In addition to direct signaling inhibition, another mechanism proposed for trastuzumab's efficacy is antibody-dependent cell cytotoxicity, mediated by natural killer (NK) cells (26). Although the mechanism of trastuzumab in slowing BT474-Gluc mammary fat pad tumors was not mediated by NK cells (Fig. S8*A*), we found a significant increase in NK cells within the brain metastatic tumor after DC101 treatment alone or with trastuzumab (Fig. S8*B*). Therefore, we tested if NK cell depletion using the NK1.1 antibody (clone PK136; BioXCell) could alter tumor response to this combination therapy. Treatment with the NK1.1 antibody for 7 d resulted in a >99% and 95% reduction in NK cells in the peripheral blood and spleen of nude mice, respectively (Fig. S8*C*). Untreated BT474-Gluc tumor growth in the brain parenchyma of nude mice was not altered due to the absence of NK cells, and the effect that the combination of trastuzumab and DC101 had on tumor growth and survival in nude mice lacking NK cells was no different from that in WT NK cell-competent nude mice (Fig. S8*D*). These findings are consistent with clinical data showing a lack of association between Fcγ receptor genotypes and trastuzumab efficacy (27). Finally, DC101 had no direct effect, either alone or in combination with trastuzumab or lapatinib, on the growth of BT474-Gluc cells in vitro (Fig. S9). Taken together, these data indicate that the enhanced benefit of the anti-HER2 and anti-VGEFR2 combination therapy in this model is not primarily due to enhanced inhibition of HER2 activity, increased NK cell-mediated cytotoxicity, or direct cytotoxicity.

Dual HER2 Targeting with Trastuzumab and Lapatinib Delays Brain Metastatic Tumor Growth Better Than Either Monotherapy. Preclinical and clinical evidence suggests the combination of trastuzumab and lapatinib acts synergistically compared to either agent alone. One report attributes this to the marked downregulation of the protein survivin, leading to enhanced tumor cell apoptosis following the combination of the two agents (28). Another report shows incomplete inhibition of the HER2 kinase after lapatinib monotherapy, and the addition of trastuzumab better suppresses HER3 phosphorylation by blocking ligand-independent interactions between HER2 and HER3 (29). In agreement, we found better growth suppression of BT474-Gluc cells in vitro with the combination compared with either monotherapy (Fig. S10*A*). Furthermore, these preclinical results are supported by clinical data in both the preoperative primary and metastatic settings (30, 31). Because these findings are limited to extracranial sites (primary and metastasis), we asked if the same tumor growth delay would occur in the brain metastasis setting. Of note, we consistently observed increased phosphorylation of HER2 in BT474-Gluc cells growing in the brain compared with the mammary fat pad (Fig. S10*B*). Although short-term (3 d) treatment with lapatinib significantly reduced HER2 phosphorylation in the brain, it could do so only to the level of that observed in the untreated mammary fat pad (Fig. S10*B*), and this effect disappeared after 15 d of treatment (Fig. S7*B*). We hypothesized that more pronounced HER2 inhibition with the combination of trastuzumab and lapatinib would be beneficial to these brain metastases with increased HER2 activation.

Consistent with the data from extracranial disease, we show a beneficial effect of combining trastuzumab and lapatinib compared with either monotherapy in our model of brain metastasis (Fig. 6*A*). Once again, we observed very little effect on tumor growth with either trastuzumab or lapatinib monotherapy, resulting in a 1.2-fold and 1.3-fold increase in median overall survival, respectively (a median of 31 d and 32 d, respectively, compared with 25 d in control-treated mice). However, the combination of two anti-HER2 agents shows a significant delay in tumor growth, leading to an increase in median survival 1.8-fold greater than in control-treated mice (44 d compared with 25 d; $P < 0.001$ compared with either monotherapy).

Triple Combination of Trastuzumab, Lapatinib, and DC101 Produces a Significant Delay in Tumor Growth and Improvement in Mouse Survival in Our Model of HER2-Positive Breast Cancer Brain Metastasis. We next examined the efficacy of combining two anti-HER2 therapies with DC101. Remarkably, we found a more dramatic tumor growth delay in mice treated with the triple combination compared with the combination treatment of any two drugs (Fig. 6*B*). This delay in tumor growth was accompanied by a dramatic increase in survival. In this particular experiment, control mice lived for a median of 22.5 d. Mice treated with the combination of trastuzumab and lapatinib lived 2.2-fold longer than control mice (a median of 49 d). Mice treated with the combination of trastuzumab and DC101 or lapatinib and DC101 lived 2.6-fold or 2.3-fold longer, respectively, than control-treated mice (a median of 58 d or 52.5 d, respectively). Meanwhile, mice treated with the triple combination lived fivefold longer than control-treated mice (a median of 113 d; $P < 0.001$ compared with any double-treatment group).

It is important to note that two of nine mice receiving triple-combination therapy were euthanized after a significant loss in weight despite their brain metastatic tumors being relatively small. The reason for this is not clear, but toxicity associated with the three-drug regimen could be involved. Additionally, although the triple combination had a dramatic effect on overall survival and the growth of the brain metastases, all tumors eventually escaped from therapy.

Discussion

Studies of HER2-positive breast cancer metastasis to the brain have been severely hampered by the lack of clinically relevant laboratory models (11, 32–34). We describe here a metastatic model that faithfully replicates the clinical response to treatment: failure of a HER2-dependent tumor growing in the brain to respond to anti-HER2 therapy. Although our direct brain parenchymal tumor implantation model lacks several earlier steps in the metastatic cascade (35), it allows for consistent tumor volume at treatment initiation as well as real-time evaluation of therapeutic efficacy using imaging and blood surrogate marker evaluation. The blood surrogate marker correlated not only with tumor volume, as estimated with intravital microscopy using the transparent cranial window model, but with tumor volume measurements made by MRI, bioluminescence, and ex vivo multispectral imaging.

The reason for the differential tumor growth and response to anti-HER2 therapy when tumors are growing at these two different sites, as observed both in our laboratory model and in

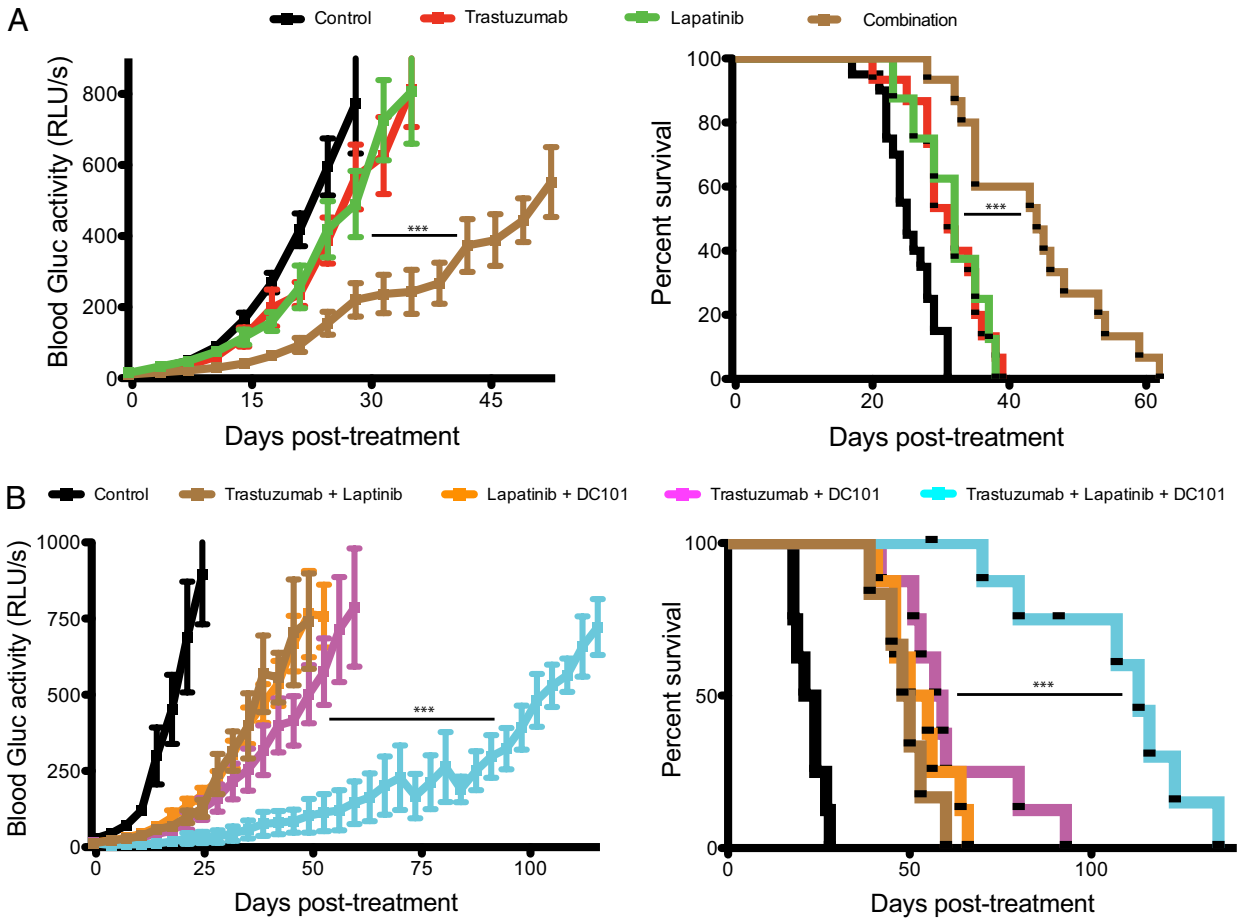

Fig. 6. Effects of dual HER2 targeting with and without anti-VEGFR2 therapy on BT474-Gluc brain metastatic tumors. (*A*) Tumor growth plot (*Left*) and Kaplan–Meier survival plot (*Right*) of tumor-bearing mice treated with control (black), trastuzumab (red), lapatinib (green), or trastuzumab and lapatinib (brown) (n = 8–20 mice). ***$P < 0.001$. (*B*) Tumor growth plot (*Left*) and Kaplan–Meier survival plot (*Right*) of tumor-bearing mice treated with control (black); trastuzumab and DC101 (magenta); lapatinib and DC101 (orange); trastuzumab and lapatinib (brown); and the triple combination of trastuzumab, lapatinib, and DC101 (cyan) (n = 6–9 mice). ***$P < 0.001$. (Final tumor growth points occur when at least three mice are still alive.)

patients, has been elusive. Surprisingly, we witnessed increased phosphorylation of HER2 in tumor cells growing in the brain compared with the mammary fat pad. This increased HER2 activity could explain a mechanism of resistance, because the reduction in phosphorylation with lapatinib treatment reached a level only equal to that of untreated mammary fat pad tumors. In addition, the effect of lapatinib disappeared after 15 d of treatment. Increased HER2 activity in the brain metastatic tumors could also explain the reason why the combination of trastuzumab and lapatinib is more beneficial than monotherapy. Future studies will be needed to test whether more intense and/or prolonged HER2 inhibition is associated with better response.

Our data provide a strong rationale for the development of anti-VEGF therapy for brain metastases from HER2-positive breast cancer. Murine VEGFR2 blockade significantly reduced tumor MVD and increased tumor necrosis and survival on its own. In combination with HER2 inhibition, VEGFR2 blockade showed an even more dramatic response. Moreover, the combination of VEGFR2 blockade with dual inhibition of HER2 showed the most impressive benefits, although there is the potential for increased toxicity. Although the exact mechanism for the triple combination is not entirely clear, we propose that the antiangiogenic benefit seen with an anti-HER2 agent and VEGFR2 blockade is synergizing with the direct tumor cell cytotoxicity induced by two anti-HER2 agents. A clinical trial studying the efficacy of carboplatin and bevacizumab in progressive breast cancer brain metastasis is currently underway (http://clinicaltrials.gov identifier NCT01004172). In this trial, patients with HER2-positive disease will also be treated with HER2 inhibitors, which may provide clinical evidence for the approach presented here. Some of these drug combinations have been previously tested in patients with *HER2*-amplified breast cancer, and there is a growing body of experience with the use of anti-VEGF therapies for primary brain tumors (12, 36). Therefore, our findings could be readily translated into the clinic to increase survival in patients with brain metastatic *HER2*-amplified breast cancer whose systemic disease is responding to therapy. Moreover, future studies will be needed to determine how these brain metastases eventually escape from this triple-combination therapy.

A recent study by our group confirmed better growth inhibition in primary breast tumors with the standard dose of DC101 (40 mg/kg) compared with lower doses, owing to a superior anti-angiogenic effect (37). However, the study also reported an added benefit of immune therapy only when combined with a low dose of DC101 (10 mg/kg), but not with the standard dose, mediated through "normalization" of the tumor vasculature. Future studies must be done to determine the optimal dose of anti-VEGFR2 therapy when combined with anti-HER2 therapies in the brain metastatic setting to achieve the greatest tumor growth delay.

Finally, it is important to mention that treatment of breast cancer brain metastases with anti-VEGF pathway therapy did

not result in an increased invasive phenotype, similar to what is observed after anti-VEGF therapy in primary brain tumors, especially after tumor hypoxia (36). Several theories could explain this phenomenon. Because BT474 cells are not invasive in nude mice, even when growing in the mammary fat pad, this phenomenon could be limited to this particular breast cancer cell line. To address this issue, future studies should investigate the invasiveness of a more aggressive breast cancer cell line when growing in the brain microenvironment after anti-VEGF therapy. Another reason for the lack of invasiveness in response to anti-VEGF therapy in our model could be because breast cancer cells do not disseminate after colonizing the brain. Could it be that the brain is the last metastatic stop for breast cancer cells, even in a hypoxic environment? If so, is this due to the unique brain microenvironment? Tracking the dissemination of breast cancer cells after growth in the brain would address this hypothesis.

Materials and Methods

Cell Lines, Infections, and Culture. BT474 cells were transduced with an expression cassette encoding Gluc and CFP separated by an internal ribosomal entry site, using a lentiviral vector as previously described (24, 38). CFP-positive BT474 cells (BT474-Gluc) were sorted with a FACSAria cell sorter (BD Biosciences). BT474-Gluc cells were maintained in RPMI 1640 supplemented with 10% (vol/vol) FBS (Atlanta Biologics).

Mammary Fat Pad and Brain Metastatic Xenografts. Female nude mice (8–9 wk of age) were ovariectomized and implanted with a 0.36-mg, 60-d release 17β-estradiol pellet (Innovative Research of America) the day before implantation of tumor cells and every 60 d thereafter. For the mammary fat pad model, 1 ± 10^6 BT474-Gluc cells were suspended in a 50-μL mixture of PBS and Matrigel Matrix High Concentration (BD Biosciences) at a 1:1 ratio before injection. For injection into the brain, the head of the mouse was fixed with a stereotactic apparatus and the skull over the left hemisphere of the brain was exposed via skin incision. Using a high-speed air-turbine drill (CH4201S; Champion Dental Products) with a burr tip size of 0.5 mm in diameter, three sides of a square (~2.5 mm in length, each side) were drilled through the skull until a bone flap became loose. Using blunt tweezers, the bone flap was pulled back, exposing the brain parenchyma. Roughly 10 μL of a BT474-Gluc cell suspension, at a concentration of 2.5×10^7 cells/mL in PBS, was injected into the brain parenchyma using an insulin syringe. The bone flap was then placed back into position in the skull and sealed using histocompatible cyanoacrylate glue, and the skin atop the skull was sutured closed. All animal procedures were performed according to the guidelines of the Public Health Service Policy on Human Care of Laboratory Animals and in accordance with a protocol approved by the Institutional Animal Care and Use Committee of Massachusetts General Hospital.

Tumor Size Monitoring and Survival Analysis. Tumor size was measured twice a week by measuring the activity of secreted Gluc in the blood. Measurement of blood Gluc was performed as described previously (24). Briefly, blood was drawn from a slight nick in a tail vein of the mouse. Thirteen microliters of blood was collected and mixed with 3 μL of 50 mM EDTA, and was then stored at −20 °C. Blood was transferred to an opaque 96-well plate, and Gluc activity was measured using coelenterazine (CTZ; Nanolight) as a substrate and a plate luminometer (Centro XS LB960; Berthold Technologies). The luminometer was set to inject 100 μL of 50 μg/mL CTZ in PBS automatically, and photon counts were acquired for 1 s. All treatments were started when the blood Gluc activity reached ~10 RLU/s, which corresponds to a tumor volume around 10 mm^3 (Fig. S1). For survival analysis, mice were euthanized when exhibiting signs of prolonged distress or neurological impairment or when they lost more than 20% of their body weight, defined as the survival end point.

Reagents and Treatments. Trastuzumab (Genentech) and lapatinib (GlaxoSmithKline) were obtained from the Massachusetts General Hospital pharmacy. Trastuzumab was administered at a concentration of 5 mg/kg body weight twice a week by i.p. injection. Each lapatinib tablet was ground and dissolved in sterile water with 0.5% Tween 80 (Sigma–Aldrich) to a concentration of 10 mg/mL and administered at a concentration of 100 mg/kg of body weight once a day by oral gavage. DC101, a generous gift from Imclone Systems (Eli Lilly and Company) was administered at a concentration of 40 mg/kg of body weight twice a week by i.p. injection. The control treatment for lapatinib was 0.5% Tween 80 (10 μL/g), the control treatment for trastuzumab was 5 mg/kg of body weight of a nonspecific human IgG (Jackson ImmunoResearch Laboratories, Inc.), and the control treatment for DC101 was 40 mg/kg of body weight of a nonspecific rat IgG (Jackson ImmunoResearch Laboratories, Inc.).

Quantification of Necrotic Tumor Area. Mouse brain with tumor tissue was cross-coronally sectioned through the center, fixed in 4% paraformaldehyde overnight, and embedded in paraffin. Ten-micometer sections were stained with H&E. Tumors were evaluated by a trained neuropathologist (M.S.), and areas of necrosis were designated. A custom-written MATLAB (MathWorks) program was used to determine the fraction of necrotic area in the tumor. The majority of tumors had a viable rim; thus, the total tumor area could be determined. The area of necrosis was then quantified with respect to the full cross-sectional tumor area.

Quantification of Blood Vessel and Lectin Perfusion Area. Before euthanasia, mice were injected with 2.5 μg of biotinylated-lectin per gram of body weight into the heart and allowed to circulate for 5 min. For immunofluorescence staining, mouse brains were fixed for 8 h in 4% (vol/vol) formaldehyde in PBS at 4 °C, followed by incubation in 30% sucrose in PBS at 4 °C for 48 h and subsequent mounting in freezing media [Optimal Cutting Temperature (OCT); Tissue-Tek]. Brains were sectioned every 20 μm. For endothelial cell identification, tissue sections were incubated overnight at 4 °C with an anti-CD31 antibody (2.5 μg/mL, clone 2H8; Millipore), followed by incubation with a 1:200 dilution of an Alexa 649-conjugated anti-Armenian hamster antibody for 1 h at room temperature. For identification of perfused blood vessels, tissue sections were incubated for 1 h at room temperature with a 1:200 dilution of Alexa 546-conjugated streptavidin. Tissues were mounted with 4′-6-diamidino-2-phenylindole–containing mounting media (Vectashield; VectorLabs). Quantification of the stained area was performed using an in-house MATLAB program.

ACKNOWLEDGMENTS. We thank S. Roberge, J. Kahn, C. Smith, N. Kirkpatrick, R. Ramjiawan, and P. Huang for help with experiments and interpretation of data, and D. Duda, B. Seed, and I. Kuter for useful suggestions and clinical insight. We also thank ImClone Systems/Eli Lilly and Company for the generous gift of DC101. This work was supported, in part, by US Department of Defense Breast Cancer Research Innovator Award W81XWH-10-1-0016 (to R.K.J.); US National Cancer Institute Grants R01-CA126642 (to R.K.J.), P01-CA080124 (to R.K.J. and D.F.), and R01-CA096915 (to D.F.); Federal Share Proton Beam Program Income (to R.K.J.); Grant T32-CA073479 (to D.P.K.); Basic Research Projects in High-tech Industrial Technology at Gwangju Institute of Science and Technology (E.C.); the Institute of Medical System Engineering at Gwangju Institute of Science and Technology (E.C.); the Bio & Medical Technology Development Program and Basic Science Program through the National Research Foundation of Korea Grants 2011-0019619 and 2012R1A1A1012853 (to E.C.) a Tosteson postdoctoral fellowship at the Massachusetts General Hospital (to E.C.); Grant R21CA155862 (to C.T.F.); and US National Institutes of Health Grant K25AG029415 (to C.T.F.).

1. Lin NU, Winer EP (2007) Brain metastases: The HER2 paradigm. *Clin Cancer Res* 13(6): 1648–1655.
2. Leyland-Jones B (2009) Human epidermal growth factor receptor 2-positive breast cancer and central nervous system metastases. *J Clin Oncol* 27(31):5278–5286.
3. Brufsky AM, et al. (2011) Central nervous system metastases in patients with HER2-positive metastatic breast cancer: Incidence, treatment, and survival in patients from registHER. *Clin Cancer Res* 17(14):4834–4843.
4. Pestalozzi B, et al. (2011) Trastuzumab does not increase the incidence of central nervous system (CNS) relapse in HER2-positive early breast cancer: The HERA trial experience. *Cancer Res* 71(24, Suppl 3):P4-17-01.
5. Palmieri D, et al. (2007) Her-2 overexpression increases the metastatic outgrowth of breast cancer cells in the brain. *Cancer Res* 67(9):4190–4198.
6. Stemmler HJ, et al. (2006) Characteristics of patients with brain metastases receiving trastuzumab for HER2 overexpressing metastatic breast cancer. *Breast* 15(2):219–225.
7. Sledge GW, Jr. (2011) HER2011: The changing face of HER2-positive breast cancer. *Clin Breast Cancer* 11(1):9.
8. Geyer CE, et al. (2006) Lapatinib plus capecitabine for HER2-positive advanced breast cancer. *N Engl J Med* 355(26):2733–2743.
9. Lin NU, et al. (2008) Phase II trial of lapatinib for brain metastases in patients with human epidermal growth factor receptor 2-positive breast cancer. *J Clin Oncol* 26(12): 1993–1999.
10. Lin NU, et al. (2009) Multicenter phase II study of lapatinib in patients with brain metastases from HER2-positive breast cancer. *Clin Cancer Res* 15(4):1452–1459.
11. Eichler AF, et al. (2011) The biology of brain metastases—Translation to new therapies. *Nat Rev Clin Oncol* 8(6):344–356.

12. Folkman J (2007) Angiogenesis: An organizing principle for drug discovery? *Nat Rev Drug Discov* 6(4):273–286.
13. Kumar S, et al. (1999) Breast carcinoma: Vascular density determined using CD105 antibody correlates with tumor prognosis. *Cancer Res* 59(4):856–861.
14. Dvorak HF (2002) Vascular permeability factor/vascular endothelial growth factor: A critical cytokine in tumor angiogenesis and a potential target for diagnosis and therapy. *J Clin Oncol* 20(21):4368–4380.
15. Miller K, et al. (2007) Paclitaxel plus bevacizumab versus paclitaxel alone for metastatic breast cancer. *N Engl J Med* 357(26):2666–2676.
16. Martín M, et al. (2012) Phase II study of bevacizumab in combination with trastuzumab and capecitabine as first-line treatment for HER-2-positive locally recurrent or metastatic breast cancer. *Oncologist* 17(4):469–475.
17. Besse B, et al. (2010) Bevacizumab safety in patients with central nervous system metastases. *Clin Cancer Res* 16(1):269–278.
18. Izumi Y, Xu L, di Tomaso E, Fukumura D, Jain RK (2002) Tumour biology: Herceptin acts as an anti-angiogenic cocktail. *Nature* 416(6878):279–280.
19. Fukumura D, et al. (1998) Tumor induction of VEGF promoter activity in stromal cells. *Cell* 94(6):715–725.
20. Harmey JH, Dimitriadis E, Kay E, Redmond HP, Bouchier-Hayes D (1998) Regulation of macrophage production of vascular endothelial growth factor (VEGF) by hypoxia and transforming growth factor beta-1. *Ann Surg Oncol* 5(3):271–278.
21. du Manoir JM, et al. (2006) Strategies for delaying or treating in vivo acquired resistance to trastuzumab in human breast cancer xenografts. *Clin Cancer Res* 12(3 Pt 1):904–916.
22. Le XF, et al. (2008) Specific blockade of VEGF and HER2 pathways results in greater growth inhibition of breast cancer xenografts that overexpress HER2. *Cell Cycle* 7(23): 3747–3758.
23. Witte L, et al. (1998) Monoclonal antibodies targeting the VEGF receptor-2 (Flk1/KDR) as an anti-angiogenic therapeutic strategy. *Cancer Metastasis Rev* 17(2):155–161.
24. Chung E, et al. (2009) Secreted Gaussia luciferase as a biomarker for monitoring tumor progression and treatment response of systemic metastases. *PLoS ONE* 4(12): e8316.
25. Konecny GE, et al. (2006) Activity of the dual kinase inhibitor lapatinib (GW572016) against HER-2-overexpressing and trastuzumab-treated breast cancer cells. *Cancer Res* 66(3):1630–1639.
26. Spector NL, Blackwell KL (2009) Understanding the mechanisms behind trastuzumab therapy for human epidermal growth factor receptor 2-positive breast cancer. *J Clin Oncol* 27(34):5838–5847.
27. Hurvitz SA, et al. (2012) Analysis of Fcγ receptor IIIa and IIa polymorphisms: Lack of correlation with outcome in trastuzumab-treated breast cancer patients. *Clin Cancer Res* 18(12):3478–3486.
28. Xia W, et al. (2005) Combining lapatinib (GW572016), a small molecule inhibitor of ErbB1 and ErbB2 tyrosine kinases, with therapeutic anti-ErbB2 antibodies enhances apoptosis of ErbB2-overexpressing breast cancer cells. *Oncogene* 24(41):6213–6221.
29. Garrett JT, et al. (2011) Transcriptional and posttranslational up-regulation of HER3 (ErbB3) compensates for inhibition of the HER2 tyrosine kinase. *Proc Natl Acad Sci USA* 108(12):5021–5026.
30. Guarneri V, et al. (2012) Preoperative chemotherapy plus trastuzumab, lapatinib, or both in human epidermal growth factor receptor 2-positive operable breast cancer: Results of the randomized phase II CHER-LOB study. *J Clin Oncol* 30(16):1989–1995.
31. Blackwell KL, et al. (2012) Overall survival benefit with lapatinib in combination with trastuzumab for patients with human epidermal growth factor receptor 2-positive metastatic breast cancer: Final results from the EGF104900 Study. *J Clin Oncol* 30(21): 2585–2592.
32. Fidler IJ (2011) The role of the organ microenvironment in brain metastasis. *Semin Cancer Biol* 21(2):107–112.
33. Cruz-Muñoz W, Kerbel RS (2011) Preclinical approaches to study the biology and treatment of brain metastases. *Semin Cancer Biol* 21(2):123–130.
34. Kienast Y, et al. (2010) Real-time imaging reveals the single steps of brain metastasis formation. *Nat Med* 16(1):116–122.
35. Bos PD, et al. (2009) Genes that mediate breast cancer metastasis to the brain. *Nature* 459:1005–1009.
36. Carmeliet P, Jain RK (2011) Molecular mechanisms and clinical applications of angiogenesis. *Nature* 473(7347):298–307.
37. Huang Y, et al. (2012) Vascular normalizing doses of antiangiogenic treatment reprogram the immunosuppressive tumor microenvironment and enhance immunotherapy. *Proc Natl Acad Sci USA* 109:17561–17566.
38. Wurdinger T, et al. (2008) A secreted luciferase for ex vivo monitoring of in vivo processes. *Nat Methods* 5(2):171–173.